Available online at www.sciencedirect.com

ScienceDirect

Geochimica et Cosmochimica Acta 215 (2017) 263–276

Geochimica et Cosmochimica Acta

www.elsevier.com/locate/gca

An integrated chemical and oxygen isotopic study of primitive olivine grains in picrites from the Emeishan Large Igneous Province, SW China: Evidence for oxygen isotope heterogeneity in mantle sources

Song-Yue Yu [a], Neng-Ping Shen [a], Xie-Yan Song [a,*], Edward M. Ripley [b,*], Chusi Li [b], Lie-Meng Chen [a]

[a] State Key Laboratory of Ore Deposit Geochemistry, Institute of Geochemistry, Chinese Academy of Sciences, Guiyang 550081, China
[b] Department of Geological Sciences, Indiana University, Bloomington, IN 47405, USA

Received 25 January 2017; accepted in revised form 31 July 2017; available online 4 August 2017

Abstract

Recognition of the nature of potential mantle sources of continental flood basalts is complicated by possible overprinting related to crustal contamination as magmas migrate to the surface (Arndt and Christensen, 1992). However, in picritic lava flows primitive olivine phenocrysts that formed early in the crystallization sequence can potentially provide unperturbed information of their mantle source. We have carried out an integrated chemical and oxygen isotopic (*in situ* SIMS) study of primitive olivine grains (Fo ranging from 88 to 92.6 mol%) in the Emeishan picrites at different locations (Wulongba, Wuguijing, Tanglanghe and Maoniuping). We use these data to evaluate the geochemical nature of mantle sources for magmas from which the primitive olivine crystallized. The primitive olivine grains in the samples from Maoniuping, Wuguijing and Tanglanghe are characterized by mantle-like $\delta^{18}O$ values (mean values are $5.1 \pm 0.3‰$ (2σ, $n = 53$), $5.2 \pm 0.3‰$ (2σ, $n = 122$) and $5.3 \pm 0.3‰$ ($n = 25$), respectively) coupled with generally low Fo contents (mean values are 88.7 ± 1.4 mol% (2σ, $n = 53$), 89.8 ± 1.8 mol% (2σ, $n = 122$) and 89.4 ± 1.8 mol% (2σ, $n = 25$), respectively). In contrast, the olivine grains in the samples from Wulongba are characterized by elevated $\delta^{18}O$ values (mean $= 5.6 \pm 0.3‰$ (2σ, $n = 58$)) coupled with generally higher Fo contents (mean $= 91 \pm 2.8$ mol% (2σ, $n = 58$)) than primitive olivine in the samples from the other locations. Based on olivine compositions, primitive olivine in picrites from Maoniuping, Tanglanghe and Wuguijing are consistent with derivation from hybrid mantle sources containing similar proportions of peridotite and pyroxenite/eclogite components. The $\delta^{18}O$ values of these primitive olivine grains are consistent with melting of plume source materials. The chemical composition of the primitive olivine from Wulongba are also consistent with derivation from a hybrid peridotite/pyroxenite source, but the high $\delta^{18}O$ values suggest that at least locally the pyroxenitic source was characterized by ^{18}O-enrichment related to a higher degree of seawater interaction with the oceanic crust protolith. An alternative explanation is that olivine in the Wulongba picrite reflects derivation from lithospheric mantle that was modified by subduction-related processes in the Neoproterozoic. The high-Fo content of the Wulongba picrites may be due to the higher fO_2 conditions of the partial melt generated in the subduction modified lithospheric mantle, or to a higher degree of partial melting.

Keywords: Olivine oxygen isotopes; Olivine chemistry; Picrites; Mantle sources; Emeishan; China

* Corresponding authors.
E-mail addresses: songxieyan@vip.gyig.ac.cn (X.-Y. Song), ripley@indiana.edu (E.M. Ripley).

http://dx.doi.org/10.1016/j.gca.2017.08.007
0016-7037/

1. INTRODUCTION

The compositional variations observed in continental flood basalt (CFB) provinces remain a poorly understood feature of igneous petrogenesis. Variations in magma compositions may be related to both deep mantle and lithospheric mantle source variability (e.g., Hawkesworth et al., 1984; Arndt and Christensen, 1992; Sobolev et al., 2007; Kamenetsky et al., 2016), variation in the depth and extent of mantle partial melting (e.g., McKenzie and Bickle, 1988; Ren et al., 2017), possible mixing of magmas derived from mantle sources (e.g., Hooper, 1985; Arndt et al., 1998; Jennings et al., 2017), and contamination involving continental crust as magma ascends to the surface (e.g., Arndt et al., 1993; Baker et al., 2000). Picritic volcanic rocks (MgO > 12 wt%, Le Bas, 2000) associated with flood basalts provide the best possibility of evaluating primitive magmas that were parental to the more voluminous basaltic rocks. However, assimilation processes and hydrothermal alteration frequently tend to mask evidence for primary compositions. If the picritic magmas were emplaced rapidly and/or avoided prolonged residence in magma chambers, then early-formed olivine should provide information regarding the nature of the mantle source. Recent studies of primitive olivine-hosted melt inclusions (Kamenetsky et al., 2012, 2016; Jennings et al., 2017; Ren et al., 2017) have been used to evaluate mantle source compositions, variability, and mixing scenarios for picrites in CFB provinces. The oxygen isotopic composition of primitive olivine phenocrysts in picritic rocks from CFB provinces has also been used to investigate source mantle heterogeneity (Bindeman and Kamenetsky, 2009; Harris et al., 2015; Heinonen et al., 2015; Kamenetsky et al., 2016). Wang et al. (2015) also utilized oxygen isotope ratios of primitive olivines in picrites to evaluate the potential role of hydrous mantle in the genesis of flood basalts.

Sobolev et al. (2005, 2007) used the composition of primitive olivine phenocrysts to evaluate the importance of magma derivation from a peridotitic mantle source relative to that of a pyroxenitic (recycled eclogitic material) source. The method employed was based primarily on the NiO, MnO and CaO contents of the olivine phenocrysts. Ren et al. (2017), using the chemical and Pb isotopic composition of melt inclusions in olivine, concluded that a secondary pyroxenite source, produced by mixing of a recycled oceanic crust component with a peridotite component, was involved in the genesis of picritic lavas.

We have used both O isotope and elemental composition data from primitive olivine in picritic lavas from the central zone of the Emeishan Large Igneous Province (ELIP, Figs. 1 and 2) to constrain the processes that may have contributed to the overall compositional variations observed in the province. Picrites from the Emeishan LIP have been divided into high-Ti (Ti/Y = 800) and low-Ti (Ti/Y = 300) end-members, with an intermediate-Ti series that forms a continuous spectrum between the two end-members (Kamenetsky et al., 2012; Ren et al., 2017; Fig. 3). Many researchers have suggested that high-Ti lavas in the ELIP were produced by deep melting of the plume materials whereas coexisting low-Ti lavas are products of shallower melting of the plume plus the overlying metasomatized lithospheric mantle (Xu et al., 2001; Xiao et al., 2004; He et al., 2010). Some researchers believe that a pyroxenite or eclogite component within the lithospheric mantle was the main source of the high-Ti lavas (Hou et al., 2011, 2012). Kamenetsky et al. (2012) suggest that the low-Ti end-member was derived from a peridotite source, whereas the high-Ti end-member was derived from a garnet pyroxenite mantle source. Ren et al. (2017) suggest that all of the Emeishan mafic lavas are derived from a pyroxenite source, with high-Ti melts reflecting lower degrees of melting at greater depths relative to the extents and depths of melting for the low-Ti melts. Other researchers have proposed that the high-Ti lavas formed by interaction of the ascending mantle plume with subducted Paleozoic oceanic crust that was trapped in the asthenosphere (Zhong et al., 2011; Bai et al., 2014). Picrites from four sample locations (Wulongba, Wuguijing, Tanglanghe and Maoniuping, Fig. 2) plot between high-Ti and low-Ti endmembers in a Ti/Y versus Gd/Yb plot (Fig. 3, see also Kamenetsky et al., 2012). In order to better constrain the possible reasons for such compositional differences we investigated variations in the oxygen isotope and chemical compositions of primitive olivine grains in picrites from these four localities. *In situ* SIMS olivine oxygen isotope analyses have not previously been done for samples from the ELIP; the method allowed us to utilize only the cores of fresh olivine grains that had been determined by electron microprobe analysis to be $>Fo_{88}$. Most samples contained zoned olivine grains with a range in Fo values from 79 to 93 mole%, consistent with variations in whole rock minor elements and attributable to fractional crystallization. Our approach has allowed us to document variations in primitive olivine O isotopic ratios and compositions that reflect melt derivation from a hybrid peridotite/pyroxenite plume-mantle source, as well as subduction-modified lithospheric mantle.

2. GEOLOGICAL BACKGROUND

The Permian Emeishan large igneous province (ELIP) is composed of voluminous flood basalts and numerous contemporaneous mafic–ultramafic intrusions. It is located in the western margin of the Yangtze Block, SW China (Fig. 1). The Yangtze Block is bounded by the Simao Block and the Tibet Plateau to the west. The Simao Block and the Tibet Plateau are Gondwana-derived micro-continents. The amalgamation of these continental blocks and the Yangtze Block took place from Late Paleozoic in the south to Early Mesozoic in the north (Deng et al., 2014). The assembly of the Yangtze and Cathaysia blocks took place during Neoproterozoic time (e.g., Li, 1999). Holistic geological records indicate that the western rim of the Yangtze Block was part of the circum-Rodinia arc system in the Neoproterozoic (Cawood et al., 2013). The eastward subduction along the western margin of the Yangtze Block during this period of time produced abundant arc igneous suites between Panzhihua and Xichang (Zhou et al., 2006), the northern reach of the ELIP (Fig. 1).

The Emeishan flood basalts are exposed in an area of more than 2.5×10^5 km^2 (Chung and Jahn, 1995; Xu

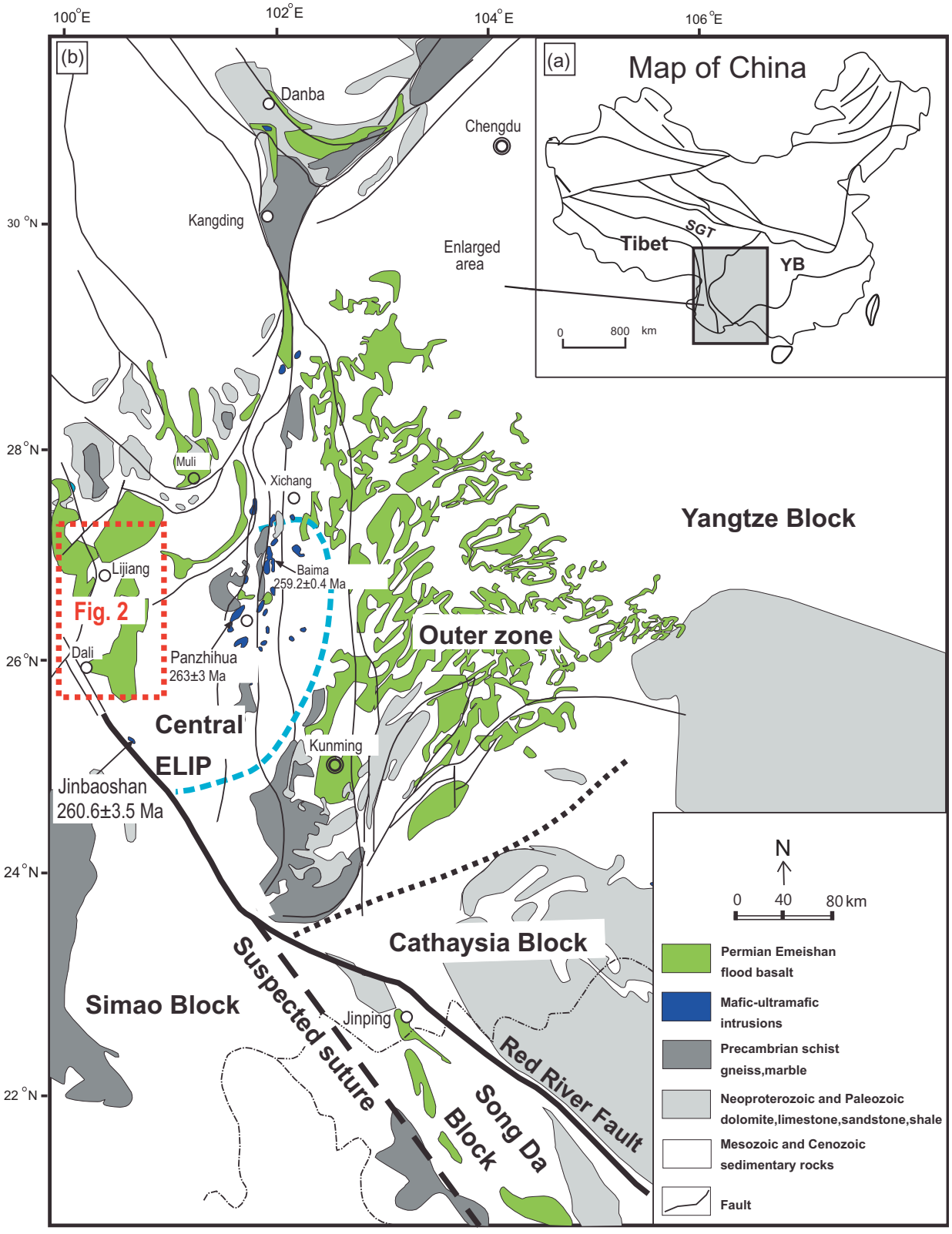

Fig. 1. Geologic map showing the simplified tectonic framework of China (a). Distribution of the late-Permian Emeishan flood basalts and coeval mafic intrusions (b), modified after Song et al. (2008) and Li et al. (2016).

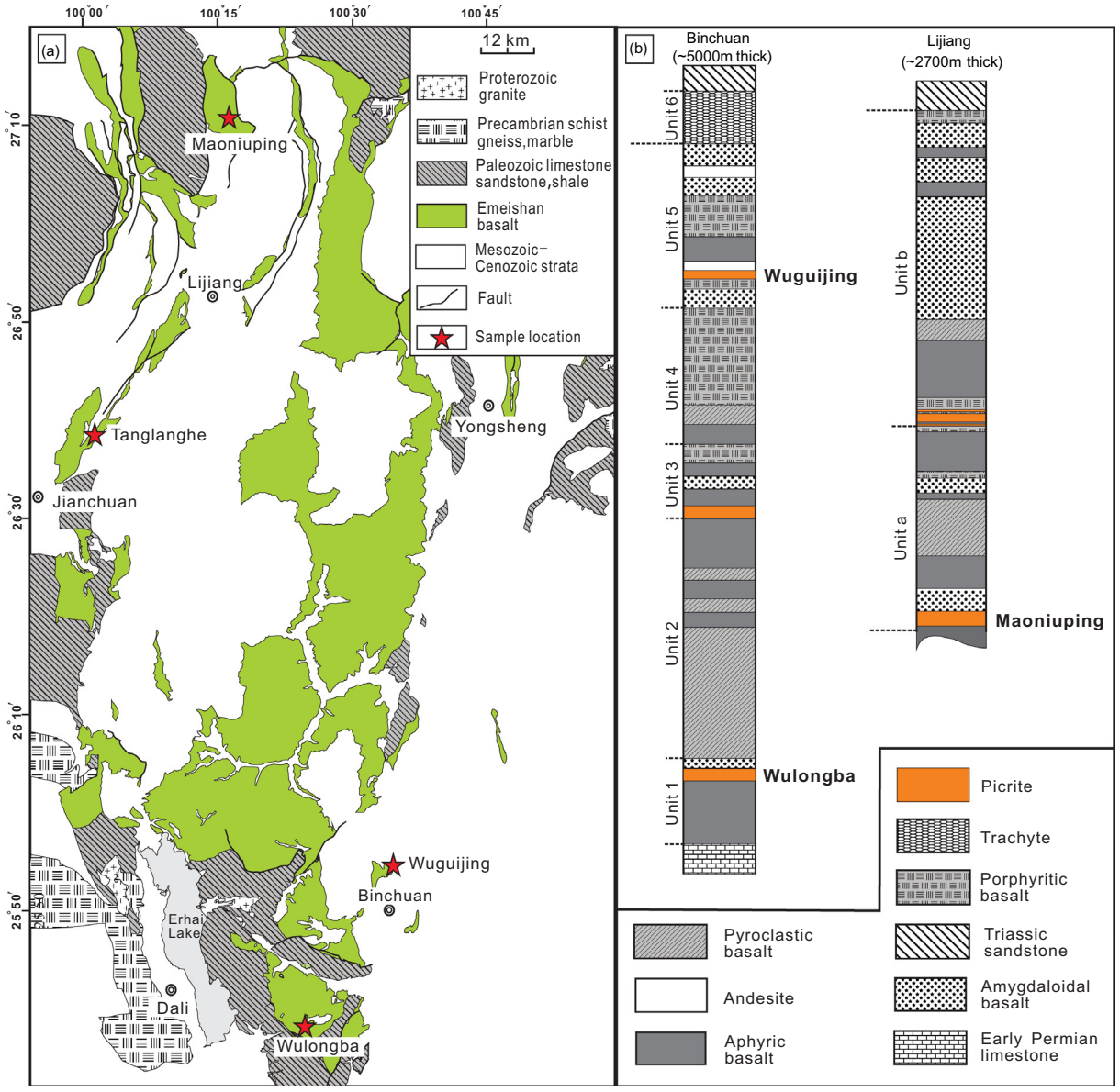

Fig. 2. Distribution of the Emeishan flood basalts in the studied area (a, after Yunnan, 1990). Stratigraphic columns at Binchuan and Lijiang area (b, modified after Xiao et al., 2004; Zhang et al., 2006).

et al., 2001; Song et al., 2001). The flood basalt province within China is further divided into the central and outer zones (Fig. 1). Both low–Ti and high–Ti basalts are important in the central zone. In contrast, the outer zone is dominated by high–Ti basalts (Xu et al., 2001; Xiao et al., 2004). Radiometric dating of associated mafic-ultramafic intrusions gives an age of magmatism at ~260 Ma for the ELIP, which is roughly contemporaneous with the global end-Guadalupian mass extinction (Ali et al., 2002; Zhou et al., 2002a). To date picritic lava flows have only been found in the central zone of the flood basalt province within China. The picritic lava flows occur in different parts of the volcanic sequences at different locations. The thicknesses of individual picritic lava flows vary from ~3 to 50 m (Xiao et al., 2004; Zhang et al., 2006, 2008; Li et al., 2010a,b, 2012).

Many coeval mafic–ultramafic intrusions with zircon U-Pb ages close to 260 Ma (e.g., Zhou et al., 2002a) are exposed in the SW part of the ELIP because of significant uplifting and erosion in this region after magma emplacement. Country rocks to these intrusions are mainly Proterozoic gneisses and schists, Neoproterozoic dolomites and Early Permian limestones. Some of these intrusions, such as Baima, Hongge, Panzhihua and Taihe host important Fe–Ti–V oxide ore deposits. A few other coeval intrusions in the region, such as Baimazhai, Limahe and Jinbaoshan, host economically valuable Ni–Cu–PGE sulfide deposits (Tao et al., 2007, 2008).

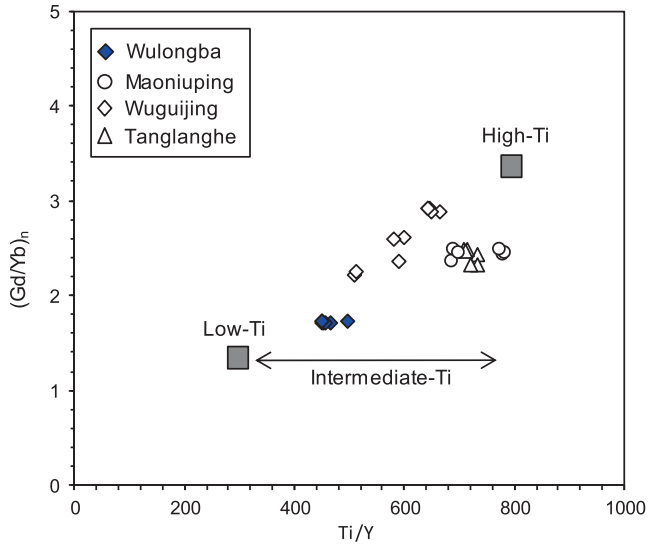

Fig. 3. Whole rock Ti/Y versus $(Gd/Yb)_n$ (normalization to the primitive mantle composition of Sun and McDonough (1989)). The classification of high-Ti, low-Ti and intermediate-Ti is after Kamenetsky et al. (2012). Whole rock data are shown in Electronic Appendix 3b.

3. SAMPLES AND ANALYTICAL METHODS

3.1. Sample descriptions

The picrite samples used in this study were collected from four different locations in the ELIP from the Dali to the Lijiang districts: Wulongba, Wuguijing, Tanglanghe and Maoniuping (Fig. 2). In outcrop, the picritic flows can be easily distinguished from the associated basaltic flows by their darker color (Fig. 4a). At Wulongba and Maoniuping, the sampled picritic lava flows occur in the lower parts of the volcanic sequences (Fig. 2b). At Wuguijing, the sampled picritic lava flow is present in the upper part of the volcanic succession. At Tanglanghe, the exact stratigraphic position of the sampled picritic flow is not clear because the outcrops in this area are limited.

Among the picrite samples used in this study, those from Wulongba are least altered (Fig. 4b). Serpentine replacement is restricted only to a small proportion of microfractures in olivine crystals. The Wulongba picrites contain about ~20–30% olivine grains of variable sizes (0.2–3 mm in diameter) and minor augite phenocrysts (<1%). Some oli-

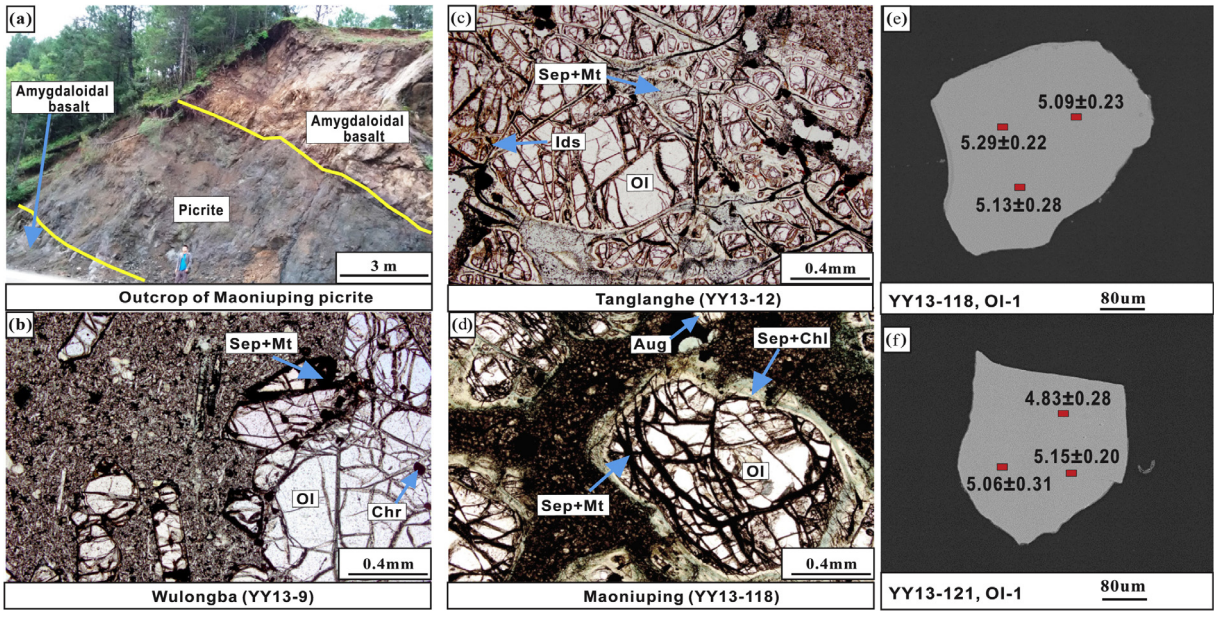

Fig. 4. Photo of a representative outcrop of an Emeishan picrite (a). Photomicrograph of representative texture of the Emeishan picrites (b–d). Back-scattered secondary electron images (e–f) displaying representative olivine grains from Maoniuping. The red square denotes the SIMS analytical spot for oxygen isotopes. Ol = olivine, Aug = augite, Chl = chlorite, Ids = iddingsite, Chr = chromite, Sep = serpentine, Mt = Magnetite. (For interpretation of the references to colour in this figure legend, the reader is referred to the web version of this article.)

vine crystals contain small Cr-spinel inclusions (50–800 μm in diameter). The fine-grained groundmass is composed of plagioclase, pyroxene and minor Fe-Ti oxides.

The picrite samples from Wuguijing are more altered than those from Wulongba, i.e., serpentine replacement along micro-fractures in olivine is more common. The picrite samples from Wuguijing similarly contain ~20–35% olivine grains. The groundmass is composed of fine-grained pyroxene and plagioclase that have been partially altered to chlorite, talc and clay minerals.

The picrite samples from Tanglanghe and Maoniuping are also more altered than those from Wulongba. The primary textures and modal compositions of the picrites from these different locations are generally similar. In the Tanglanghe picrites, disseminated iddingsite is present between serpentine veins and residual olivine kernels (Fig. 4c). In addition to serpentine replacement along micro-fractures in olivine, the Maoniuping picrites are also characterized by an alteration band composed of serpentine and chlorite wrapping around most olivine crystals (Fig. 4d).

3.2. Analytical methods

The Emeishan picrite samples were crushed manually to pieces <0.5 mm in diameter (Fig. 4e). Olivine grains were hand-picked using a binocular microscope. The selected grains were mounted in epoxy and polished. Microphotographs under both transmitted and reflected light were used to select grains with inclusion-free large cores for chemical analysis by electron microprobe. The back-scattered electron (BSE) images (Fig. 4f) were used for target selection during *in situ* oxygen isotope analysis by secondary ion mass spectrometry (SIMS).

The *in situ* oxygen isotope analysis of olivine was carried out using a CAMECA IMS-1280 ion microprobe in the Institute of Geology and Geophysics, Chinese Academy of Sciences (IGGCAS), Beijing, China. The analytical procedures, instrument conditions, calibration and data reduction are the same as given in Li et al. (2010). Results are presented in standard delta notation:

$$\delta^{18}O = (({}^{18}O/{}^{16}O)_{sample}/({}^{18}O/{}^{16}O)_{standard}) - 1$$

Values are given in ‰ relative to the Vienna Standard Mean Ocean Water standard via multiplication of the delta value by 1000. For the SIMS analyses a Cs^+ primary beam was accelerated at 10 kV with an intensity of ~2 nA. The beam size was about 10 × 20 μm. An electron gun was used to compensate for sample charging during analysis. Each analysis took ~4 min, consisting of pre-sputtering (~120 s), automatic beam centering and integration of oxygen isotopes (10 cycles × 4 s, total 40 s), which gave an average internal precision of 0.2‰ (2SE). Multiple grains of a San Carlos olivine standard (Fo ~ 90 mole%) were mounted together with our samples for analysis. No grain-to-grain variability in forsterite content was revealed by multiple electron probe microanalyses (EPMA). Our olivine samples were run during two analytical sessions: 4 days in May 2014 and 3 days in August 2016 (Electronic Appendix 1). Analytical sessions were monitored in term of drift and precision using two bracketing standards (San Carlos olivine) for every four-sample analyses. Measured $^{18}O/^{16}O$ was normalized using the Vienna Standard Mean Ocean Water composition (VSMOW, $^{18}O/^{16}O = 0.0020052$). In this study, olivine phenocrysts selected for oxygen isotope analysis range in forsterite content from ~88 to 93 mol%, which is very close to the forsterite content (~90) of the San Carlos olivine standard used during analysis. Instrumental mass fractionation was corrected following the procedure described in Li et al. (2010) using the San Carlos olivine standard with a recommended value of 5.4 ± 0.2‰ (2σ, $n = 20$) determined previously by conventional fluorination in the Stable Isotope Research Facility of Indiana University. Experience from the Cameca IMS 1280 lab at the IGGCAS and other labs worldwide indicates that matrix effects resulting from variable Mg# in olivine on the measured oxygen isotope ratios is not significant, provided that the olivine is characterized by Fo values ranging from 60 to 100 (Bindeman et al., 2008; Kita et al., 2009; Wang et al., 2015; Harris et al., 2015). For example, Bindeman et al. (2008) observed a systematic difference of instrumental mass fractionation (IMF) for San Carlos (Fo_{90}) and CI114 (Fo_{74}) olivines of 0.12‰, which translates to 0.0075‰ of IMF per each Fo number. Accordingly, difference of IMF for olivine phenocrysts used in this study ($Fo_{88\text{-}93}$) is less than 0.04‰, which is negligible and within error of our measurements. After elimination of extreme data points outside of two sigma values, sixty-three measurements of San Carlos olivine grains during the first analytical session (in May 2014) and seventy-five measurements of San Carlos olivine grains during the second analytical session (in August 2016) gave identical average external precision (~0.2‰, 2σ, Electronic Appendix 1, Fig. 5a). The 2σ standard deviation on duplicate analyses of individual olivine grains from unknown samples was better than 0.3‰ (Fig. 4e and f, Electronic Appendix 1). The analytical results are shown in Electronic Appendix 2.

The major and trace element compositions of olivine were determined by wavelength-dispersive X-ray emission microanalysis using a CAMECA SX50 electron microprobe in the Department of Geological Sciences at Indiana University. Analytical conditions for major elements were 15 keV accelerating voltage, 20 nA beam current, 1 μm beam size and peak counting time of 20 s. Mn and Ni in olivine were analyzed using a beam current of 100 nA and a peak counting time of 100 s. Under these conditions the detection limits were estimated to be 64 ppm Mn and 99 ppm Ni. Matrix effects were corrected using the PAP program supplied by CAMECA. Analytical uncertainty was within ±2% of accepted values, based on the results from the San Carlos olivine standard (USNM 1113122/444) analyzed together with our samples. The analytical results are shown in Electronic Appendix 2.

4. RESULTS

4.1. Oxygen isotope compositions of primitive olivine grains

The oxygen isotope compositions of the Emeishan primitive olivine grains having Fo > 88 mol% are listed in Electronic Appendix 2. The differences of replicated analyses for

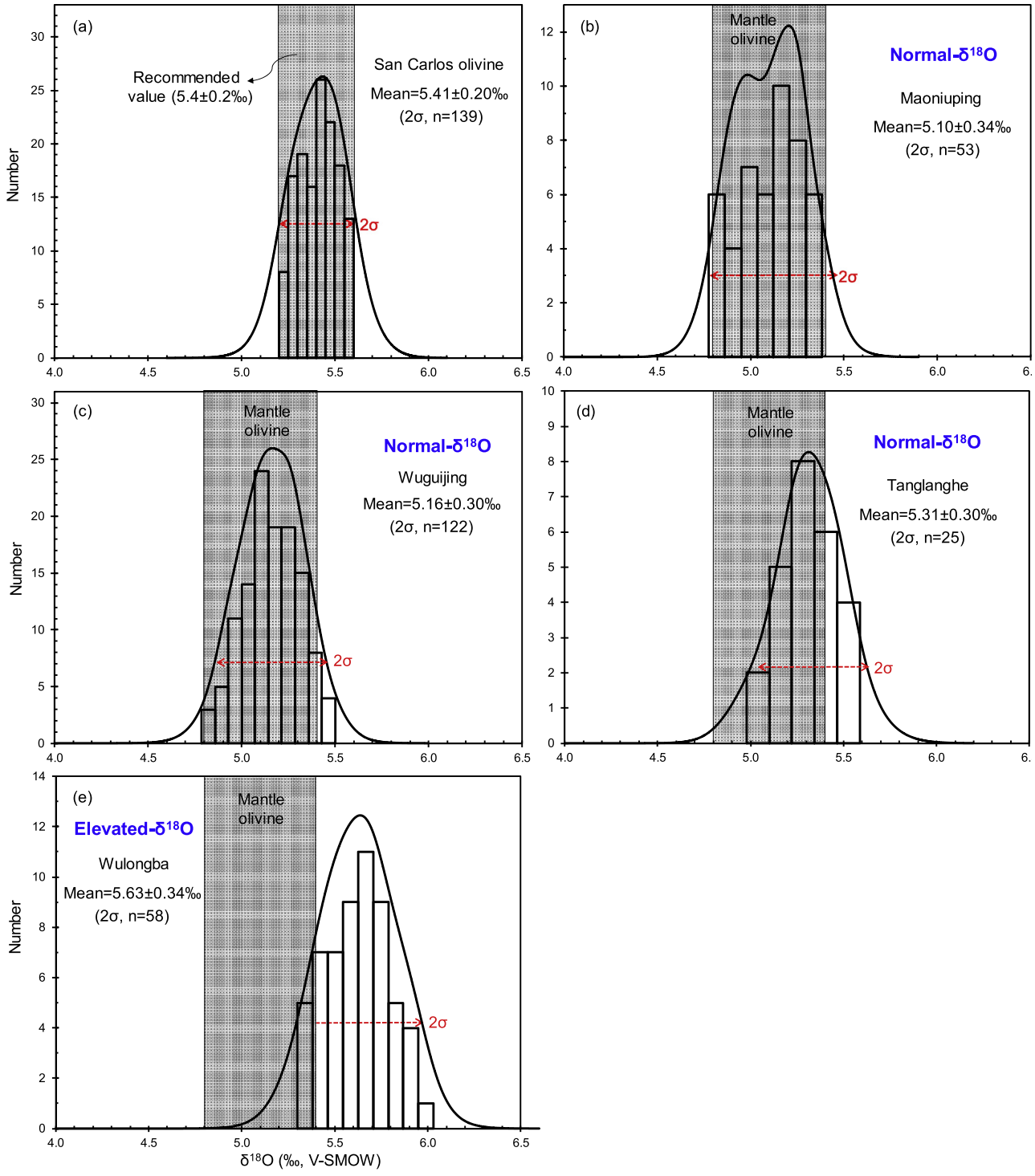

Fig. 5. Oxygen isotope composition of primitive olivine grains (Fo > 88) analyzed by SIMS. The analytical results for the multiple grains of San Carlos olivine standard are also shown. Oxygen isotope compositions of mantle olivine (4.8–5.4‰) are after Mattey et al. (1994).

a single grain with similar Fo contents in the same session are 0.2–0.3‰, which is similar to the range of typical analytical uncertainty (Electronic Appendix 1, Fig. 4e and f). The $\delta^{18}O$ values for all the picrite samples used in this study are between 4.8 and 6.0‰.

The primitive olivine grains in the picrites from Maoniuping and Wuguijing have $\delta^{18}O$ values from 4.8 to 5.5‰ with mean values of 5.1 ± 0.3‰ (2σ, $n = 53$) and 5.2 ± 0.3‰ (2σ, $n = 122$), respectively (Fig. 5b and c). The primitive olivine grains in the picrites from Tanglanghe

have $\delta^{18}O$ values between 5.0 and 5.7‰ with a mean value of 5.3 ± 0.3‰ (2σ, $n = 25$) (Fig. 5d). The oxygen isotope compositions of olivine grains from the above three localities are similar to those typically assigned to those of mantle origin (Mattey et al., 1994). The primitive olivine grains in the picrites from Wulongba have the highest $\delta^{18}O$ values from 5.3 to 6.0‰ with a mean value of 5.6 ± 0.3‰ (2σ, $n = 58$) (Fig. 5e).

4.2. Olivine Mg-Fe-Ni-Mn systematics

The chemical compositions of the primitive olivine grains that have been determined for oxygen isotope compositions are listed in Electronic Appendix 2. The Fo contents of the primitive olivine grains from the different samples used in this study overlap, but the elevated-$\delta^{18}O$ primitive olivine grains in the picrites from Wulongba tend to have higher Fo contents (Fig. 6a). The normal-$\delta^{18}O$ primitive olivine grains in pircites from Maoniuping, Wuguijing and Tanglanghe tend to have lower Fo contents (Fig. 6a). At a given Fo content, the contents of Ni and Mn in the elevated-$\delta^{18}O$ primitive olivine phenocrysts in the picrites from Wulongba are similar to the other types of olivine (Fig. 6a and b). The contents of Ni and Mn in the different types of the Emeishan olivine phenocrysts are much higher and lower, respectively, than those of olivine found to crystallize from experimental peridotite-derived melts (Fig. 6a and b, Sobolev et al., 2007). In the diagrams of 100Mn/Fe versus 100Ni/Mg and Ni/(Mg/Fe)/1000, the different types of the Emeishan olivine phenocrysts mostly plot between those of olivines found to crystallize from experimental peridotite-derived melts and from experimental pyroxenite-derived melts (Fig. 6c and d, Sobolev et al., 2007). In the diagram of olivine $\delta^{18}O$ versus Fo (Fig. 6e), the olivine phenocrysts in the samples from Wulongba are characterized by higher Fo and $\delta^{18}O$ values compared with those from other localities. No clear correlation between $\delta^{18}O$ and Fo contents is present for a single type of olivine. Moreover, no clear correlation between $\delta^{18}O$ and Mn/Fe is present for a single type of olivine or all types of olivine as a whole (Fig. 6f).

5. DISCUSSION

There are several possibilities for the significant oxygen isotope variations of the primitive olivine grains with Fo > 88 mole% from the Emeishan picrites (Fig. 5). These include (1) analytical uncertainty during SIMS analysis, (2) processes associated with partial melting, (3) fractional crystallization, (4) post-magmatic hydrothermal alteration, (5) variable crustal contamination and (6) source variation. The range of $\delta^{18}O$ values (4.8–6.0‰) for primitive olivine grains from Emeishan picritic samples is partially related to the analytical uncertainty of SIMS (0.2–0.3‰, 2σ). The grain to grain oxygen isotope variation within a single hand sample is typically between 0.2 and 0.3‰ (2σ, Electronic Appendix 2), similar to the analytical uncertainties of SIMS. This suggests no detectable oxygen isotope variation for olivine grains within a single hand sample. We thus use a mean $\delta^{18}O$ value of multiple olivine grains from an individual sample to represent the "true" oxygen isotope composition of this sample (Electronic Appendix 2). These mean values range from 5.0 to 5.7‰, and can be regarded as the oxygen isotope variation for primitive olivine from the Emeishan picritic lavas. The mean $\delta^{18}O$ values (5.6–5.7‰) for primitive olivine phenocrysts from Wulongba (Fig. 5e, Electronic Appendix 2) are much higher than those from other localities (5.0–5.4‰). This difference cannot be attributed to analytical uncertainty. Olivine-melt fractionation is very small at high temperatures (<0.1‰, e.g., Chiba et al., 1989; Eiler, 2001), and therefore processes related to partial melting or fractional crystallization could not be responsible for the large difference between the $\delta^{18}O$ values of olivine from Wulongba and those from other localities. The other three possibilities are evaluated below.

5.1. Post-magmatic alteration

Interaction between olivine and hydrothermal fluids caused variable serpentinization along micro-fractures (Fig. 4). Oxygen isotope exchange at 100 °C–400 °C (a typical temperature range of serpentinization, Wenner and Taylor, 1971) with assumed low-^{18}O fluids (0 to −15‰ - similar to the $\delta^{18}O$ values of modern meteoric water or sea water), will cause progressive ^{18}O depletion in olivine. The mantle-like $\delta^{18}O$ values for the main group of primitive olivine grains from Maoniuping, Tanglanghe and Wuguijing (Fig. 5b–d) likely represent their original oxygen isotope compositions at magmatic temperatures and are not thought to have been affected by post-eruption hydrothermal alteration. The elevated $\delta^{18}O$ values for primitive olivine grains from Wulongba (Fig. 5e) are less likely related to fluid-olivine isotope exchange, in part because ^{18}O enrichment for olivine is only possible during interaction with high ^{18}O-fluids (>3‰) at low temperatures (<100 °C). However, oxygen diffusion rates at low temperatures are extremely slow (Reddy et al., 1980). A more direct line of evidence against hydrothermal alteration causing the observed elevated $\delta^{18}O$ values for primitive olivine grains from Wulongba is that the primitive olivine from these samples show no signs of more extensive alteration than those containing olivine with mantle-like $\delta^{18}O$ values. For example, a high-^{18}O olivine from Wulongba (Figs. 4b and 5e), is the least serpentinized among all of the samples used in this study. In addition, as the oxygen isotope compositions of the primitive olivine grains in the samples were determined by an in situ method the analytical targets in the selected primitive olivine grains were always away from micro-fractures (Electronic Appendix 4). Finally, the variation of observed $\delta^{18}O$ values for different spots with different distances from nearby micro-fractures is within the analytical uncertainty (Electronic Appendix 4). Therefore, we conclude that post-magmatic hydrothermal alteration is not a primary cause for the observed mantle-like or elevated $\delta^{18}O$ values for the primitive olivine grains in the Emeishan picrites.

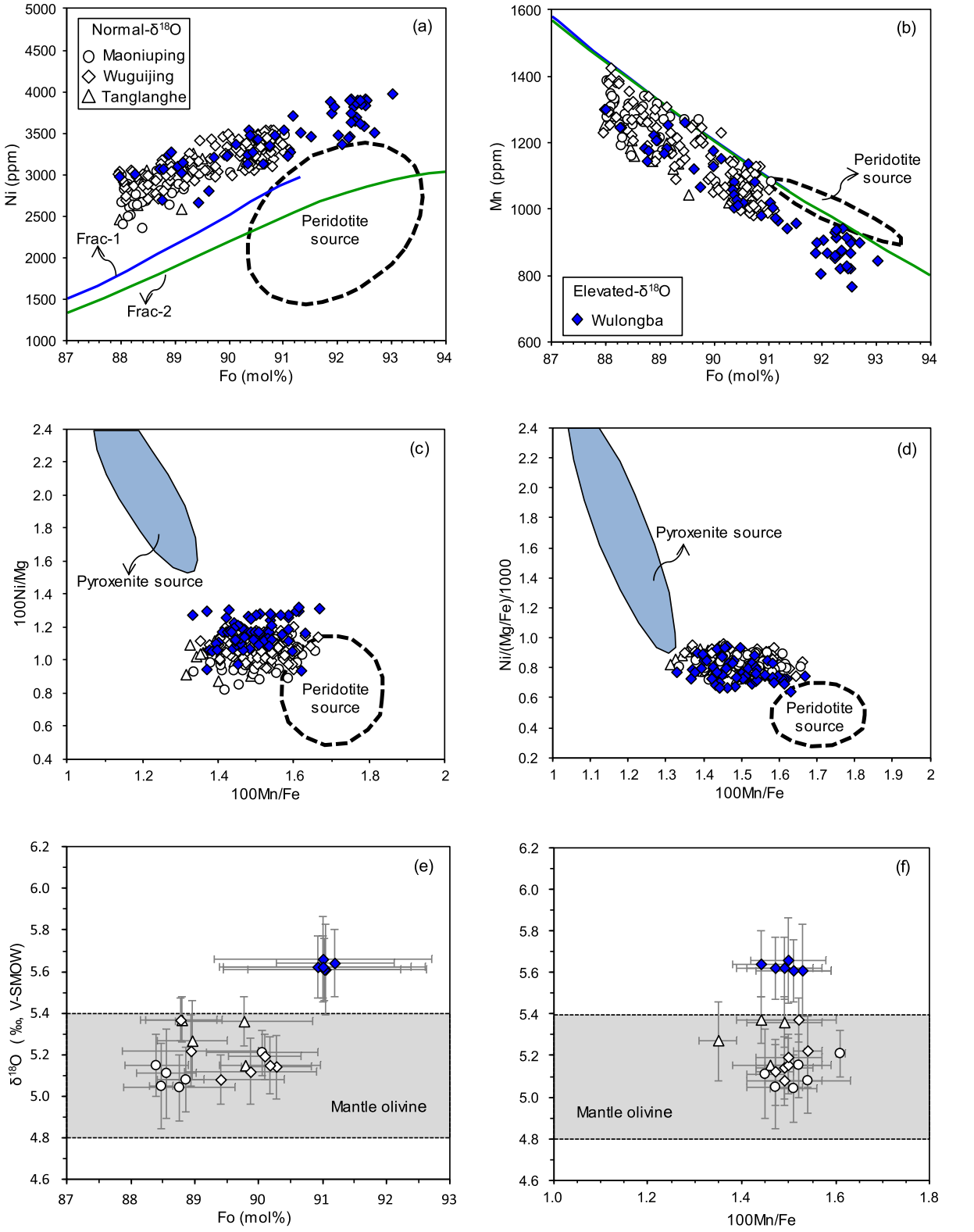

Fig. 6. Chemical compositions of primitive olivine grains (Fo > 88) from the Emeishan picrites. Plot of Fo versus Ni and Mn (a–b). Plot of 100 Mn/Fe against 100Ni/Mg and Ni/(Mg/Fe)/1000 (c–d). Plots of mean $\delta^{18}O_{olivine}$ values versus mean Fo contents and 100 Mn/Fe ratios in each individual sample (e–f). Error bars given represent two standard deviations. Olivine compositions corresponding to peridotite and pyroxenite sources are after Sobolev et al. (2007). Frac-1 and Frac-2 are two trends of olivine compositions during fractional crystallization from melts derived from fertile peridotite at 3 Gpa, 1515 °C and at 4 Gpa, 1630 °C, respectively (after Sobolev et al., 2007).

5.2. Crustal contamination

The elevated olivine $\delta^{18}O$ values from Wulongba are unlikely to have resulted from contamination with siliceous crustal materials (e.g., chert, turbidites, felsic igneous rocks and gneisses) because such contaminants have very low contents of MgO (e.g., Plank and Langmuir, 1998) and would dilute the MgO content of the magma resulting in crystallization of olivine with a lower Fo value. This is not consistent with the high-Fo contents for olivine phenocrysts from Wulongba compared with those from other localities (Fig. 6e).

Tang et al. (2017) reported an increase of Mg content coupled with a decrease of Ni content in olivine as the result of brucite marble assimilation (addition of Mg but not Ni) by magma in the Panzhihua picritic dyke of the Emeishan LIP. Because the $\delta^{18}O$ values of brucite marbles (7–28‰, Ganino et al., 2013; Yu et al., 2015) are significantly higher than mantle-derived magma, marble assimilation by magma would cause both elevated Fo and $\delta^{18}O$ values for primitive olivine grains. This would also be the case if the assimilant was Mg-rich or dolomitic carbonate. However, the higher Ni values for olivine phenocrysts from Wulongba compared with those from other localities (Fig. 6c) are not consistent with carbonate assimilation alone.

5.3. Source control

It has been suggested that mantle source heterogeneity is a primary control on oxygen isotope variations of primitive olivine grains in OIB and LIP picrites (e.g., Eiler et al., 1996, 1997, 2000; Skovgaard et al., 2001; Bindeman et al., 2006, 2008; Day et al., 2009; Day et al., 2010; Gurenko et al., 2011; Harris et al., 2015; Heinonen et al., 2015; Kamenetsky et al., 2016). Primitive olivine grains with mantle-like $\delta^{18}O$ values in OIB and LIP picrites have unanimously been attributed to a peridotite source by these authors. However, different opinions exist for the primitive olivine grains with $\delta^{18}O$ values that deviate from the mantle values. In the Hawaiian, Society and Samoan islands, primitive olivine grains having elevated $\delta^{18}O$ values (ranging from 5.4 to 6.1‰) were attributed to the presence of recycled sediments and/or oceanic basalts with a low-temperature history in the plume source (Eiler et al., 1996, 1997). In the Canary Islands the primitive olivine grains having elevated $\delta^{18}O$ values (up to 6.0‰) were thought to result from the involvement of a pyroxenite component derived from recycled oceanic upper crust during magma generation (Gurenko et al., 2011). In the Karoo LIP, primitive olivine grains having elevated $\delta^{18}O$ values (ranging from 6.0 to 6.7‰) also were attributed to the presence of pyroxenite/eclogite components (Harris et al., 2015; Kamenetsky et al., 2016) during magma generation. As shown in Fig. 6c and d, all different types of primitive olivine phenocrysts in the Emeishan picrites can be explained by derivation from hybrid mantle sources containing similar proportions of peridotite and pyroxenite/eclogite components (Sobolev et al., 2007). Both the olivine chemistry reported here and the results of chemical and Pb isotopic analyses of melt inclusions from picrites in the Emeishan flood basalt province (Ren et al., 2017) are consistent with a significant component of pyroxenite in the source region of the picrites. Unfortunately, uncertainties in the oxygen isotopic composition of end members prevent a rigorous evaluation of potential mixing mechanisms. Kamenetsky et al. (2012) estimated that the intermediate- and high-Ti magmas of the Emeishan province contained 21 and 47%, respectively, of a garnet pyroxenite component in the mantle source. If the peridotitic component of the mantle were characterized by a $\delta^{18}O$ value of 5.0‰, then 20% mixing with a pyroxenitic source of 6.0‰ would produce a source with a $\delta^{18}O$ value of 5.2‰, a value consistent with the oxygen isotope ratios of picrites from Maoniuping, Tanglanghe and Wuguijing. In the case of the low-Ti Wulongba picrites a similar contribution of pyroxenitic material seems unlikely, unless the end member components were characterized by very different $\delta^{18}O$ values. This is certainly conceivable if the oceanic crust that was the source of the pyroxenitic component for the Wulongba area had interacted more strongly with seawater, and was therefore characterized by a more elevated $\delta^{18}O$ value. Rather than speculate on variations in $\delta^{18}O$ values of source components we offer an alternative explanation for the chemical and isotopic composition of the Wulongba picrites.

Previous studies have demonstrated that island arc lavas and lithospheric mantle beneath subduction zones commonly display an ^{18}O-enriched character (Eiler et al., 1998; Dorendorf et al., 2000; Bindeman et al., 2005; Chen and Zhou, 2005; Auer et al., 2009; Liu et al., 2014). For example, olivine phenocrysts from Kamchatka arc lavas commonly show elevated $\delta^{18}O$ values (5.1–7.6‰) which may be derived from ^{18}O-enriched metasomatized lithospheric mantle (Dorendorf et al., 2000; Auer et al., 2009). ^{18}O-enriched olivine and pyroxene crystals ($\delta^{18}O$ ranging from 4.5 to 7.0 and 6.2 to 10.3‰, respectively) and enclosing melt inclusions ($\delta^{18}O$ ranging from 8.8 to 12.2‰) in peridotite xenoliths from lithospheric mantle above the Manus-Kilinailau subduction zone suggest that the sub-arc mantle wedge is characterized by elevated $\delta^{18}O$ values (Eiler et al., 1998). Elevated $\delta^{18}O$ values of olivine (~8‰) and pyroxene (6.9‰) in mantle xenoliths from South Tibet and the North China Craton, respectively, were considered to represent derivation from ^{18}O-enriched lithospheric mantle produced as a result of subduction-related metasomatism (Chen and Zhou, 2005; Liu et al., 2014). The Emeishan picritic lavas were erupted in the late Permian (Fig. 1, Tang et al., 2015) at the western margin of the Yangtze Block. The nature of lithospheric mantle beneath this region during this time period is poorly known because of the absence of mantle xenoliths in the ELIP. However, previous studies have demonstrated that subduction of oceanic lithosphere occurred to the east, underneath the Yangtze Block in the Neoproterozoic, as indicated by abundant subduction-related igneous rocks in the region with zircon U-Pb ages varying from ~860 Ma to ~760 Ma (e.g., Zhou et al., 2002b, 2006). We speculate that lithospheric mantle in this region has elevated $\delta^{18}O$ values because of subduction-related metasomatism in the Neoproterozoic.

We propose that lithospheric mantle previously modified by subduction processes was heated by a mantle plume in the Permian and underwent large degrees of partial melting. Products included picritic magmas from which olivine with elevated $\delta^{18}O$ values crystallized (such as the primitive olivine in picrite samples from Wulongba). Partial melting in the deeper mantle produced picritic magmas from which olivine with more typical mantle $\delta^{18}O$ values, such as those in the picrites from Maoniuping, Wuguijing and Tanglanghe, crystallized. A subtle alternative to produce the high-^{18}O olivines from Wulongba is mixing involving plume-derived picritic magma and high degree, high-^{18}O partial melts from the lithosphere.

The higher Fo contents for olivine phenocrysts from Wulongba compared with those from other localities could originate via two different mechanisms. One relates to the premise that the oxidation state of magmas derived from subduction modified lithospheric mantle would be higher than that of deeper plume-derived magmas. Previous studies have demonstrated that the oxidation state of plume-derived magmas generally lie at the QFM (quartz-fayalite-magnetite) buffer or somewhat more reducing (e,g., Carmichael and Ghiorso, 1986; Rhodes and Vollinger, 2005). In contrast, the oxidation state of arc basalts derived from the sub-arc mantle wedge are typically at QFM+1 to +1.6, significantly more oxidized than basalts from other tectonic settings (e.g., Kelley and Cottrell, 2012). The oxidation state of lithospheric mantle beneath the western Yangtze Block in the late Permian is unknown, but we suggest that lithospheric mantle in this region was oxidized due to subduction in the Neoproterozoic. In the late Permian, this subduction-modified lithospheric mantle began to melt due to plume-lithosphere interaction and produced oxidized melts. The more oxidized magmas were characterized by relatively low $Fe^{2+}/Fe^{3+}$and higher MgO/FeO at constant Mg and total Fe contents; crystallization of high Fo olivine could have resulted. The second mechanism that could explain the high Fo content of olivine from Wulongba is different degrees of partial melting of the subduction modified lithospheric mantle. High degrees of partial melting of this source could have produced melts with high MgO/FeO, with crystallization of high-Fo olivine from picritic magmas. The relative importance of these two mechanisms for producing high-Fo olivines such as those in the picrites from Wulongba remains to be determined.

6. CONCLUSIONS

The range of oxygen isotope compositions for primitive olivine in picrites from the ELIP is from 5.0 to 5.7‰, larger than the range typically assigned to olivine of mantle origin (4.8–5.4‰). Primitive olivine grains with mantle-like $\delta^{18}O$ values are present in the samples from Maoniuping, Tanglanghe and Wuguijing. Primitive olivine grains with elevated $\delta^{18}O$ values are present in samples from Wulongba. The primitive olivine grains in these samples tend to have higher Fo contents than those in samples from elsewhere in the Emeishan flood basalt province. Based on olivine chemistry primitive olivine in all of the Emeishan picrites may have been derived from hybrid mantle sources containing similar proportions of peridotite and pyroxenite/eclogite components. The primitive olivine grains in the picrites from Wulongba were derived from an ^{18}O-enriched source, but one whose chemical composition did not perturb olivine Fe-Mg-Ni-Mn systematics. Although these features are consistent with the involvement of a pyroxenitic source that locally was characterized by particularly elevated $\delta^{18}O$ values, we propose that the high-^{18}O olivine in the Wulongba picrite more likely reflects derivation from lithospheric mantle that was modified by subduction-related processes in the Neoproterozoic. The high-Fo content of the Wulongba picrites may be due to the higher fO_2 conditions of the partial melt generated in the subduction modified lithospheric mantle, or to a higher degree of partial melting.

ACKNOWLEDGMENTS

We thank Prof. Xian-Hua Li and Dr. Xiao-Xiao Ling of the Institute of Geology and Geophysics, Chinese Academy of Sciences for their guidance in in-situ oxygen isotope analysis by SIMS. This study was funded by the strategic priority research program (B) of the Chinese Academy of Sciences (XDB18000000), the National Key Research and Development Program of China (2016YFC0600502), NSFC (41573009, 41373042, 41473024), Open Research Fund of the State Key Laboratory of Ore Deposit Geochemistry of China (SKLODG grant #201204). We greatly appreciate constructive comments from Professor Chris Harris and two anonymous reviewers. Professor Marc Norman and Professor Weidong Sun provided diligent editorial handling.

APPENDIX A. SUPPLEMENTARY MATERIAL

Supplementary data associated with this article can be found, in the online version, at http://dx.doi.org/10.1016/j.gca.2017.08.007.

REFERENCES

Ali J. R., Thompson G. M., Song X. and Wang Y. (2002) Emeishan basalts (SW China) and the 'end-Guadalupian'crisis: magnetobiostratigraphic constraints. *J. Geol. Soc.* **159**, 21–29.

Arndt N., Chauvel C., Czamanske G. and Fedorenko V. (1998) Two mantle sources, two plumbing systems: tholeiitic and alkaline magmatism of the Maymecha River basin, Siberian flood volcanic province. *Contrib. Mineral. Petrol.* **133**, 297–313.

Arndt N. T. and Christensen U. (1992) The role of lithospheric mantle in continental flood volcanism: Thermal and geochemical constraints. *J. Geophys. Res.: Solid Earth* **97**, 10967–10981.

Arndt N. T., Czamanske G. K., Wooden J. L. and Fedorenko V. A. (1993) Mantle and crustal contributions to continental flood volcanism. *Tectonophysics* **223**, 39–52.

Auer S., Bindeman I., Wallace P., Ponomareva V. and Portnyagin M. (2009) The origin of hydrous, high-$\delta^{18}O$ voluminous volcanism: diverse oxygen isotope values and high magmatic water contents within the volcanic record of Klyuchevskoy volcano, Kamchatka, Russia. *Contrib. Mineral. Petrol.* **157**, 209–230.

Bai Z.-J., Zhong H., Li C., Zhu W.-G., He D.-F. and Qi L. (2014) Contrasting parental magma compositions for the Hongge and Panzhihua magmatic Fe-Ti-V oxide deposits, Emeishan Large Igneous Province, SW China. *Econ. Geol.* **109**, 1763–1785.

Baker J., Macpherson C., Menzies M., Thirlwall M., Al-Kadasi M. and Mattey D. (2000) Resolving crustal and mantle contributions to continental flood volcanism, Yemen; constraints from mineral oxygen isotope data. *J. Petrol.* **41**, 1805–1820.

Bindeman I., Gurenko A., Sigmarsson O. and Chaussidon M. (2008) Oxygen isotope heterogeneity and disequilibria of olivine crystals in large volume Holocene basalts from Iceland: Evidence for magmatic digestion and erosion of Pleistocene hyaloclastites. *Geochim. Cosmochim. Acta* **72**, 4397–4420.

Bindeman I. and Kamenetsky V. (2009) *The Mantle Sources of Continental Flood Basalts from Oxygen Isotope Composition of Primitive Olivine Phenocrysts*. Goldschmidt Abstracts, Davos, Switzerland, p. A123.

Bindeman I., Sigmarsson O. and Eiler J. (2006) Time constraints on the origin of large volume basalts derived from O-isotope and trace element mineral zoning and U-series disequilibria in the Laki and Grímsvötn volcanic system. *Earth Planet. Sci. Lett.* **245**, 245–259.

Bindeman I. N., Eiler J. M., Yogodzinski G. M., Tatsumi Y., Stern C. R., Grove T. L., Portnyagin M., Hoernle K. and Danyushevsky L. V. (2005) Oxygen isotope evidence for slab melting in modern and ancient subduction zones. *Earth Planet. Sci. Lett.* **235**, 480–496.

Carmichael I. S. E. and Ghiorso M. S. (1986) Oxidation-reduction relations in basic magma: a case for homogeneous equilibria. *Earth Planet. Sci. Lett.* **78**, 200–210.

Cawood P. A., Wang Y., Xu Y. and Zhao G. (2013) Locating South China in Rodinia and Gondwana: A fragment of greater India lithosphere? *Geology* **41**, 903–906.

Chen L.-H. and Zhou X.-H. (2005) Subduction-related metasomatism in the thinning lithosphere: Evidence from a composite dunite-orthopyroxenite xenolith entrained in Mesozoic Laiwu high-Mg diorite, North China Craton. *Geochem. Geophys. Geosyst.* **6**, Q06008.

Chiba H., Chacko T., Clayton R. N. and Goldsmith J. R. (1989) Oxygen isotope fractionations involving diopside, forsterite, magnetite, and calcite: Application to geothermometry. *Geochim. Cosmochim. Acta* **53**, 2985–2995.

Chung S.-L. and Jahn B.-M. (1995) Plume-lithosphere interaction in generation of the Emeishan flood basalts at the Permian-Triassic boundary. *Geology* **23**, 889–892.

Day J. M. D., Pearson D. G., Macpherson C. G., Lowry D. and Carracedo J.-C. (2009) Pyroxenite-rich mantle formed by recycled oceanic lithosphere: Oxygen-osmium isotope evidence from Canary Island lavas. *Geology* **37**, 555–558.

Day J. M. D., Pearson D. G., Macpherson C. G., Lowry D. and Carracedo J. C. (2010) Evidence for distinct proportions of subducted oceanic crust and lithosphere in HIMU-type mantle beneath El Hierro and La Palma, Canary Islands. *Geochim. Cosmochim. Acta* **74**, 6565–6589.

Deng J., Wang Q., Li G., Li C. and Wang C. (2014) Tethys tectonic evolution and its bearing on the distribution of important mineral deposits in the Sanjiang region, SW China. *Gondwana Res.* **26**, 419–437.

Dorendorf F., Wiechert U. and Wörner G. (2000) Hydrated sub-arc mantle: a source for the Kluchevskoy volcano, Kamchatka/Russia. *Earth Planet. Sci. Lett.* **175**, 69–86.

Eiler J. M. (2001) Oxygen isotope variations of basaltic lavas and upper mantle rocks. *Rev. Mineral. Geochem.* **43**, 319–364.

Eiler J. M., Grönvold K. and Kitchen N. (2000) Oxygen isotope evidence for the origin of chemical variations in lavas from Theistareykir volcano in Iceland's northern volcanic zone. *Earth Planet. Sci. Lett.* **184**, 269–286.

Eiler J. M., McInnes B., Valley J. W., Graham C. M. and Stolper E. M. (1998) Oxygen isotope evidence for slab-derived fluids in the sub-arc mantle. *Nature* **393**, 777–781.

Eiler J. M., Farley K. A., Valley J. W., Hauri E., Craig H., Hart S. R. and Stolper E. M. (1997) Oxygen isotope variations in ocean island basalt phenocrysts. *Geochim. Cosmochim. Acta* **61**, 2281–2293.

Eiler J. M., Farley K. A., Valley J. W., Hofmann A. W. and Stolper E. M. (1996) Oxygen isotope constraints on the sources of Hawaiian volcanism. *Earth Planet. Sci. Lett.* **144**, 453–467.

Ganino C., Harris C., Arndt N. T., Prevec S. A. and Howarth G. H. (2013) Assimilation of carbonate country rock by the parent magma of the Panzhihua Fe-Ti-V deposit (SW China): evidence from stable isotopes. *Geosci. Front.* **4**, 547–554.

Gurenko A. A., Bindeman I. N. and Chaussidon M. (2011) Oxygen isotope heterogeneity of the mantle beneath the Canary Islands: insights from olivine phenocrysts. *Contrib. Mineral. Petrol.* **162**, 349–363.

Harris C., le Roux P., Cochrane R., Martin L., Duncan A. R., Marsh J. S., le Roex A. P. and Class C. (2015) The oxygen isotope composition of Karoo and Etendeka picrites: High $\delta^{18}O$ mantle or crustal contamination? *Contrib. Mineral. Petrol.* **170**, 8.

Hawkesworth C. J., Marsh J. S., Duncan A. R., Erlank A. J. and Norry M. J. (1984) The role of continental lithosphere in the generation of the Karoo volcanic rocks: evidence from combined Nd- and Sr-isotope studies. In *Petrogenesis of the volcanic rocks of the Karoo Province*, 13 (ed. A. J. Erlank). Special Publication of Geological Society of South Africa, Johannesburg, pp. 341–354.

He Q., Xiao L., Balta B., Gao R. and Chen J. (2010) Variety and complexity of the Late-Permian Emeishan basalts: reappraisal of plume–lithosphere interaction processes. *Lithos* **119**, 91–107.

Heinonen J. C., Luttinen A. V. and Whitehouse M. J. (2015) *Oxygen Isotopic Evidence from Karoo Flood Basalt Olivines for Metasomatism of the Sub-Gondwanan Upper Mantle*. Goldschmidt Abstracts, Prague, p. 1223.

Hooper P. R. (1985) A case of simple magma mixing in the Columbia River Basalt Group: The Wilbur Creek, Lapwai, and Asotin flows, Saddle Mountains Formation. *Contrib. Mineral. Petrol.* **91**, 66–73.

Hou T., Zhang Z., Encarnacion J., Santosh M. and Sun Y. (2012) The role of recycled oceanic crust in magmatism and metallogeny: Os–Sr–Nd isotopes, U-Pb geochronology and geochemistry of picritic dykes in the Panzhihua giant Fe–Ti oxide deposit, central Emeishan large igneous province, SW China. *Contrib. Mineral. Petrol.* **165**, 805–822.

Hou T., Zhang Z., Ye X., Encarnacion J. and Reichow M. K. (2011) Noble gas isotopic systematics of Fe-Ti oxide ore-related mafic-ultramafic layered intrusions in the Panxi area, China: The role of recycled oceanic crust in their petrogenesis. *Geochim. Cosmochim. Acta* **75**, 6727–6741.

Jennings E. S., Gibson S. A., Maclennan J. and Heinonen J. S. (2017) Deep mixing of mantle melts beneath continental flood basalt provinces: Constraints from olivine-hosted melt inclusions in primitive magmas. *Geochim. Cosmochim. Acta* **196**, 36–57.

Kamenetsky V. S., Chung S. L., Kamenetsky M. B. and Kuzmin D. V. (2012) Picrites from the Emeishan Large Igneous Province, SW China: a compositional continuum in primitive magmas and their respective mantle sources. *J. Petrol.* **53**, 2095–2113.

Kamenetsky V. S., Maas R., Kamenetsky M. B., Yaxley G. M., Ehrig K., Zellmer G. F., Bindeman I. N., Sobolev A. V., Kuzmin D. V., Ivanov A. V., Woodhead J. and Schilling J.-G. (2016) Multiple mantle sources of continental magmatism: Insights from "high-Ti" picrites of Karoo and other large igneous provinces. *Chem. Geol.*, 10.1016/j.chemgeo.2016.08.034.

Kelley K. A. and Cottrell E. (2012) The influence of magmatic differentiation on the oxidation state of Fe in a basaltic arc magma. *Earth Planet. Sci. Lett.* **329–330**, 109–121.

Kita N. T., Ushikubo T., Fu B. and Valley J. W. (2009) High precision SIMS oxygen isotope analysis and the effect of sample topography. *Chem. Geol.* **264**, 43–57.

Le Bas M. (2000) IUGS reclassification of the high-Mg and picritic volcanic rocks. *J. Petrol.* **41**, 1467–1470.

Li C., Ripley E. M., Tao Y. and Hu R. (2016) The significance of PGE variations with Sr–Nd isotopes and lithophile elements in the Emeishan flood basalt province from SW China to northern Vietnam. *Lithos* **248–251**, 1–11.

Li C., Tao Y., Qi L. and Ripley E. M. (2012) Controls on PGE fractionation in the Emeishan picrites and basalts: Constraints from integrated lithophile–siderophile elements and Sr–Nd isotopes. *Geochim. Cosmochim. Acta* **90**, 12–32.

Li J., Xu J.-F., Suzuki K., He B., Xu Y.-G. and Ren Z.-Y. (2010) Os, Nd and Sr isotope and trace element geochemistry of the Muli picrites: Insights into the mantle source of the Emeishan Large Igneous Province. *Lithos* **119**, 108–122.

Li X. H. (1999) U-Pb zircon ages of granites from the southern margin of the Yangtze Block: timing of Neoproterozoic Jinning: Orogeny in SE China and implications for Rodinia assembly. *Precambrian Res.* **97**, 43–57.

Li X.-H., Li W.-X., Li Q.-L., Wang X.-C., Liu Y. and Yang Y.-H. (2010) Petrogenesis and tectonic significance of the ~ 850 Ma Gangbian alkaline complex in South China: Evidence from in situ zircon U-Pb dating, Hf–O isotopes and whole-rock geochemistry. *Lithos* **114**, 1–15.

Liu C.-Z., Wu F.-Y., Chung S.-L., Li Q.-L., Sun W.-D. and Ji W.-Q. (2014) A 'hidden' 18O-enriched reservoir in the sub-arc mantle. *Sci. Rep.* **4**, 4232.

Mattey D., Lowry D. and Macpherson C. (1994) Oxygen isotope composition of mantle peridotite. *Earth Planet. Sci. Lett.* **128**, 231–241.

McKenzie D. and Bickle M. J. (1988) The volume and composition of melt generated by extension of the lithosphere. *J. Petrol.* **29**, 625–679.

Plank T. and Langmuir C. H. (1998) The chemical composition of subducting sediment and its consequences for the crust and mantle. *Chem. Geol.* **145**, 325–394.

Reddy K., Oh S., Major L. and Cooper A. (1980) Oxygen diffusion in forsterite. *J. Geophys. Res.* **85**, 322–326.

Ren Z.-Y., Wu Y.-D., Zhang L., Nichols A. R. L., Hong L.-B., Zhang Y.-H., Zhang Y., Liu J.-Q. and Xu Y.-G. (2017) Primary magmas and mantle sources of Emeishan basalts constrained from major element, trace element and Pb isotope compositions of olivine-hosted melt inclusions. *Geochim. Cosmochim. Acta* **208**, 63–85.

Rhodes J. M. and Vollinger M. J. (2005) Ferric/ferrous ratios in 1984 Mauna Loa lavas: a contribution to understanding the oxidation state of Hawaiian magmas. *Contrib. Mineral. Petrol.* **149**, 666–674.

Skovgaard A. C., Storey M., Baker J., Blusztajn J. and Hart S. R. (2001) Osmium–oxygen isotopic evidence for a recycled and strongly depleted component in the Iceland mantle plume. *Earth Planet. Sci. Lett.* **194**, 259–275.

Sobolev A. V., Hofmann A. W., Kuzmin D. V., Yaxley G. M., Arndt N. T., Chung S. L., Danyushevsky L. V., Elliott T., Frey F. A., Garcia M. O., Gurenko A. A., Kamenetsky V. S., Kerr A. C., Krivolutskaya N. A., Matvienkov V. V., Nikogosian I. K., Rocholl A., Sigurdsson I. A., Sushchevskaya N. M. and Teklay M. (2007) The amount of recycled crust in sources of mantle-derived melts. *Science* **316**, 412–417.

Sobolev A. V., Hofmann A. W., Sobolev S. V. and Nikogosian I. K. (2005) An olivine-free mantle source of Hawaiian shield basalts. *Nature* **434**, 590–597.

Song X.-Y., Zhou M.-F., Hou Z.-Q., Cao Z.-M., Wang Y.-L. and Li Y. (2001) Geochemical Constraints on the Mantle Source of the Upper Permian Emeishan Continental Flood Basalts, Southwestern China. *Int. Geol. Rev.* **43**, 213–225.

Song X.-Y., Zhou M.-F., Tao Y. and Xiao J.-F. (2008) Controls on the metal compositions of magmatic sulfide deposits in the Emeishan large igneous province, SW China. *Chem. Geol.* **253**, 38–49.

Sun, S.S., McDonough, W.F., 1989. Chemical and isotopic systematics of oceanic basalts: implications for mantle composition and processes. In: Saunders, A.D., Norry, M.J., (Eds.), Magmatismin the Ocean Basins. Geological Society Special Publication, 42, pp. 313–345.

Tang Q., Li C., Tao Y., Ripley E. M. and Xiong F. (2017) Association of Mg-rich Olivine with Fe-Ti oxides as a result of carbonate assimilation by basaltic magma in the Emeishan Large Igneous Province, SW China. *J. Petrol.*. http://dx.doi.org/10.1093/petrology/egx031.

Tang Q., Li C., Zhang M. and Lin Y. (2015) U-Pb age and Hf isotopes of zircon from basaltic andesite and geochemical fingerprinting of the associated picrites in the Emeishan large igneous province, SW China. *Mineral. Petrol.* **109**, 103–114.

Tao Y., Li C., Hu R., Ripley E., Du A. and Zhong H. (2007) Petrogenesis of the Pt–Pd mineralized Jinbaoshan ultramafic intrusion in the Permian Emeishan Large Igneous Province, SW China. *Contrib. Mineral. Petrol.* **153**, 321–337.

Tao Y., Li C., Song X.-Y. and Ripley E. (2008) Mineralogical, petrological, and geochemical studies of the Limahe mafic–ultramatic intrusion and associated Ni–Cu sulfide ores, SW China. *Mineral. Deposita* **43**, 849–872.

Wang, X.-C., Wilde, S.A., Li, Q.-L., Yang, Y.-N., 2015. Continental flood basalts derived from the hydrous mantle transition zone. Nature Commun., 6.

Wenner D. B. and Taylor H. P. (1971) Temperatures of serpentinization of ultramafic rocks based on O^{18}/O^{16} fractionation between coexisting serpentine and magnetite. *Contrib. Mineral. Petrol.* **32**, 165–185.

Xiao L., Xu Y. G., Mei H. J., Zheng Y. F., He B. and Pirajno F. (2004) Distinct mantle sources of low-Ti and high-Ti basalts from the western Emeishan large igneous province, SW China: implications for plume-lithosphere interaction. *Earth Planet. Sci. Lett.* **228**, 525–546.

Xu Y., Chung S.-L., Jahn B.-M. and Wu G. (2001) Petrologic and geochemical constraints on the petrogenesis of Permian-Triassic Emeishan flood basalts in southwestern China. *Lithos* **58**, 145–168.

Yu S.-Y., Song X.-Y., Ripley E. M., Li C., Chen L.-M., She Y.-W. and Luan Y. (2015) Integrated O-Sr–Nd isotope constraints on the evolution of four important Fe–Ti oxide ore-bearing mafic–ultramafic intrusions in the Emeishan large igneous province, SW China. *Chem. Geol.* **401**, 28–42.

Yunnan, 1990. Regional geology of Yunnan province. Geological Memoirs, Series, 21. Geologic Press, Beijing (in Chinese).

Zhang Z., Mahoney J. J., Mao J. and Wang F. (2006) Geochemistry of picritic and associated basalt flows of the western Emeishan flood basalt province, China. *J. Petrol.* **47**, 1997–2019.

Zhang Z., Zhi X., Chen L., Saunders A. D. and Reichow M. K. (2008) Re-Os isotopic compositions of picrites from the Emeishan flood basalt province, China. *Earth Planet. Sci. Lett.* **276**, 30–39.

Zhong H., Qi L., Hu R.-Z., Zhou M.-F., Gou T.-Z., Zhu W.-G., Liu B.-G. and Chu Z.-Y. (2011) Rhenium-osmium isotope and

platinum-group elements in the Xinjie layered intrusion, SW China: Implications for source mantle composition, mantle evolution, PGE fractionation and mineralization. *Geochim. Cosmochim. Acta* **75**, 1621–1641.

Zhou M., Ma Y., Yan D., Xia X., Zhao J. and Sun M. (2006) The Yanbian Terrane (Southern Sichuan Province, SW China): A Neoproterozoic arc assemblage in the western margin of the Yangtze Block. *Precambrian Res.* **144**, 19–38.

Zhou M.-F., Malpas J., Song X.-Y., Robinson P. T., Sun M., Kennedy A. K., Lesher C. M. and Keays R. R. (2002a) A temporal link between the Emeishan large igneous province (SW China) and the end-Guadalupian mass extinction. *Earth Planet. Sci. Lett.* **196**, 113–122.

Zhou M.-F., Yan D.-P., Kennedy A. K., Li Y. and Ding J. (2002b) SHRIMP U-Pb zircon geochronological and geochemical evidence for Neoproterozoic arc-magmatism along the western margin of the Yangtze Block, South China. *Earth Planet. Sci. Lett.* **196**, 51–67.

Associate editor: Weidong Sun